

Quantifying the performance of jet definitions for kinematic reconstruction at the LHC

Matteo Cacciari, Juan Rojo and Gavin P. Salam

LPTHE,

UPMC – Paris 6,

Paris-Diderot – Paris 7,

CNRS UMR 7589, Paris, France

Gregory Soyez

Brookhaven National Laboratory, Upton, NY, USA

Abstract:

We present a strategy to quantify the performance of jet definitions in kinematic reconstruction tasks. It is designed to make use exclusively of physical observables, in contrast to previous techniques which often used unphysical Monte Carlo partons as a reference. It is furthermore independent of the detailed shape of the kinematic distributions. We analyse the performance of 5 jet algorithms over a broad range of jet-radii, for sources of quark jets and gluon jets, spanning the energy scales of interest at the LHC, both with and without pileup. The results allow one to identify optimal jet definitions for the various scenarios. They confirm that the use of a small jet radius ($R \simeq 0.5$) for quark-induced jets at moderate energy scales, $\mathcal{O}(100 \text{ GeV})$, is a good choice. However, for gluon jets and in general for TeV scales, there are significant benefits to be had from using larger radii, up to $R \gtrsim 1$. This has implications for the span of jet-definitions that the LHC experiments should provide as defaults for searches and other physics analyses.

Contents

1	Introduction	2
2	Analysis chain	3
2.1	Event generation	3
2.2	Jet definitions	3
2.3	Event selection and analysis	4
2.4	Figures of merit	5
2.5	Quantitative interpretation of figures of merit	6
3	Results without pileup	8
4	Results with pileup	14
4.1	Area-based pileup subtraction	15
4.2	Results	15
5	Conclusions	21

1 Introduction

A recurring question in jet studies is “what is the best jet definition for a given specific analysis”? One approach to answering such a question is to repeat the analysis for a large range of jet definitions and selecting the best, whatever this means in the context of the given analysis. This can be rather time consuming. Furthermore, experiments may not have easy access to a sufficiently large array of jet definitions — for example only a handful may be calibrated and included as standard in event records. It is therefore important to have advanced knowledge about the types and the span of jet definitions that are likely to be optimal, independently of details of specific analyses.

In this paper we investigate the question of identifying optimal jet definitions with the help of characterisations of jet-finding “quality” that are designed to be robust and physical, as well as reasonably representative of a jet definition’s quality for kinematic reconstruction tasks. We concentrate on kinematic reconstructions (rather than more QCD-oriented measurements, such as the inclusive-jet spectrum), because they are a key element in a wide range of LHC investigations, including top-quark studies and new-particle searches. We already presented in [1] a similar, though less systematic and extensive, investigation.

The quality of a given jet definition may depend significantly on the process under consideration, *i.e.* how the jets are produced. Here we will examine both quark and gluon-induced jets, spanning a range of energies. They will be obtained from Monte Carlo production and decay of fictitious narrow Z' and H bosons, with $Z' \rightarrow q\bar{q}$ and $H \rightarrow gg$. For each generated event we will cluster the event into jets with about 50 different jet definitions and determine the invariant mass of the sum of the two hardest jets. The distribution of invariant masses should then have a peak near the heavy boson mass. We will take the sharpness of that peak to be indicative of the quality of each jet definition. By scanning a range of Z', H masses we will establish this information for a range of partonic energies. $Z' \rightarrow q\bar{q}$ and $H \rightarrow gg$ events are comparatively simple, perhaps overly so, therefore we will complement them with studies of fully hadronic decays of $t\bar{t}$ events.

Our approach differs crucially from usual investigations of jet-definition quality in that it avoids any matching to unphysical Monte Carlo partons, whose relation to the jets can depend as much on

the details of the Monte Carlo showering algorithm (for example its treatment of recoil) as on the jet definition. A reflection of this is that in modern tools such as MC@NLO [2] and POWHEG [3], which include exact NLO corrections, the original Monte Carlo parton does not even exist.

A further issue that we address relates to the measurement of the sharpness of the peak. Past approaches have involved, for example, fitting a Gaussian to the peak (see *e.g.* [4, 5]) and then using its standard deviation as the quality measure. This (and related methods) are however quite unsuited to the range of peak shapes that arise, and we will therefore devise strategies for measuring peak-quality independently of the precise peak shape.

The results presented in the sections below, without pileup in section 3 and with pileup in section 4, are complemented by an interactive web-site [6], which collects a far broader range of plots than can be shown here.

2 Analysis chain

2.1 Event generation

We consider the following processes in pp collisions at 14 TeV centre of mass energy: $q\bar{q} \rightarrow Z' \rightarrow q\bar{q}$, as a source of quark jets with well-defined energies, for values of $M_{Z'}$ from 100 GeV to 4 TeV; $gg \rightarrow H \rightarrow gg$ as a source of gluons jets (as done also by Büge et al. in [1]), in a similar mass range; and fully hadronic $t\bar{t}$ events with $M_t = 175$ GeV and $M_W = 80.4$ GeV, as an example of a more complex environment.

For the Z' and H samples, the heavy-boson width has been set to (a fictitious value) of less than 1 GeV so as to produce a δ -like peak for ideal mass reconstruction, or equivalently so as to provide a mono-energetic source of jets. One should be aware also that the span of masses used here does not correspond to a physically sensible range for real Higgs or Z' bosons. This is not an issue, insofar as we are only interested in the Higgs and Z' as well-defined sources of quarks and gluons in Monte Carlo studies. To emphasise this fact, in what follows we shall refer simply to the “ $q\bar{q}$ ” and “ gg ” processes.

All the samples have been generated with Pythia 6.410 [7] with the DWT tune [8]. For the $t\bar{t}$ samples the B mesons have been kept stable.

2.2 Jet definitions

A jet definition [1] is the combination of a jet algorithm, its parameters (*e.g.* the radius R) and choice of recombination scheme. It fully specifies a mapping from particles to jets.

We will study the following infrared and collinear-safe jet algorithms:

1. the longitudinally invariant inclusive k_t algorithm [9, 10, 11], a sequential-recombination algorithm whose distance measure is the relative transverse momentum between particles.
2. The Cambridge/Aachen (C/A) algorithm [12, 13], also a sequential-recombination algorithm, which uses the rapidity-azimuth separation between particles as its distance measure.
3. The anti- k_t algorithm [14], yet another sequential-recombination algorithm, with the property that it produces conical jets (akin to an iterative cone algorithm with progressive removal, such as the current CMS cone algorithm, but without the corresponding collinear unsafety issues).

4. SISCone [15], a seedless-cone type algorithm with a split–merge step, whose overlap threshold is set to $f = 0.75$.¹ Additionally, we use the default choices of an infinite number of passes and no p_T -cut on stable cones.
5. C/A with filtering (see below).

In each case, we will add four-momenta using E -scheme (4-vector) recombination. The algorithms all have a parameter R , the jet radius, which controls the opening angle of the jets in the rapidity–azimuth plane. Results will be quite sensitive to the choice of R and we will vary it over a suitable range for each process.

In the case of the C/A algorithm, whose clustering sequence is ordered in rapidity–azimuth distance (\sim emission angle), we will also consider the impact of a filtering procedure [17] in which, subsequent to the jet finding, each jet is unclustered down to subjects at angular scale $x_{\text{filt}}R$ and one retains only the n_{filt} hardest of the subjects. We use $x_{\text{filt}} = 0.5$ and $n_{\text{filt}} = 2$. Filtering is designed to limit sensitivity to the underlying event while retaining the bulk of perturbative radiation. It is a new technique and our scope is not to investigate it in depth (for instance by also varying x_{filt} and n_{filt}), but rather to examine its potential beyond its original context.

All the jet algorithms have been used in the implementations and/or plugins of the `FastJet` package [18, 19], version 2.3, with the exception of C/A with filtering, which will be made public in a forthcoming `FastJet` release.

2.3 Event selection and analysis

For each event in the $q\bar{q}$ and gg processes, the reconstruction procedure is the following:

1. Carry out the jet finding using all final-state particles, taking the definition of hadron level proposed as standard in [1].
2. Keep only events in which the two hardest jets have $p_T \geq 10 \text{ GeV}$, $|y| \leq 5$ and rapidity difference $|\Delta y| \leq 1$ (the last of these conditions ensures that the corresponding hard partons cover a limited range of transverse momenta, close to $M/2$).
3. Reconstruct the invariant mass of the two hardest jets.

For the fully hadronic $t\bar{t}$ process:

1. Carry out the jet finding as above.
2. Keep only events in which the 6 hardest jets have $p_T \geq 10 \text{ GeV}$ and $|y| \leq 5$, and of which exactly two are b -tagged (*i.e.* contain one or more B -hadrons).
3. Using the four non b -tagged jets, consider the 3 possible groupings into two pairs (*i.e.* two candidate W -bosons). For each grouping, calculate the invariant mass of each pair of jets and keep the grouping that minimises $(M_{i_1 i_2} - M_W)^2 + (M_{i_3 i_4} - M_W)^2$.
4. Reconstruct the invariant masses for the two top quarks by pairing the b and W jets. The ambiguity in the bW pairing is resolved by taking the solution that minimises the mass difference between the two candidate top quarks.

¹The value of f has been chosen to avoid the “monster-jets” [16] that can appear with a previously common default of $f = 0.5$.

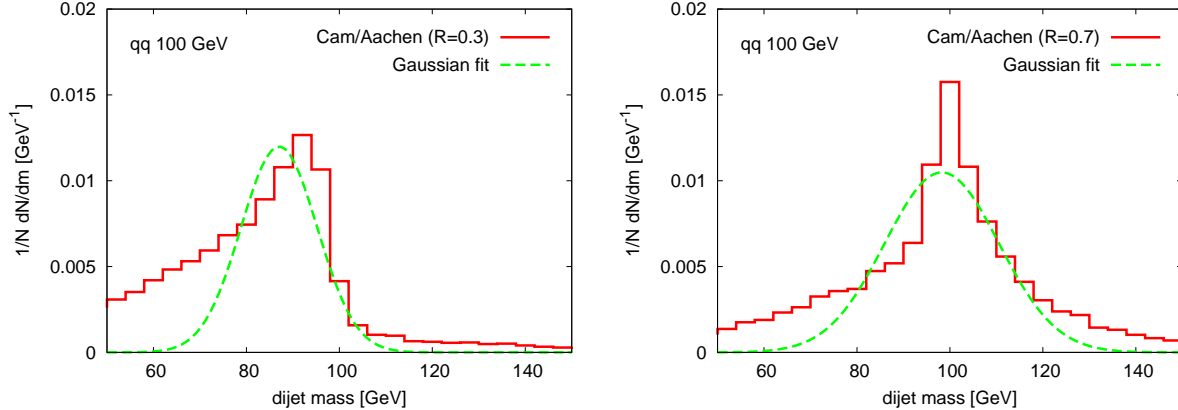


Figure 1: The dijet mass distribution for $q\bar{q}$ events with $M_{q\bar{q}} = 100$ GeV, compared to a Gaussian fitted for reconstructed dijet masses between 75 and 125 GeV, for two jet definitions: Cambridge/Aachen with $R = 0.3$ (left) and $R = 0.7$ (right).

Note that we do not pass the events through any form of detector simulation. However the choices of quality-measures that we use to study the invariant-mass distributions will, in part, take into account known detector resolutions.

2.4 Figures of merit

The above procedure will give us invariant mass distributions for each $q\bar{q}$ (*i.e.* Z'), and gg (H) mass (and for W and top in the $t\bar{t}$ sample) and for each jet definition. We next need to establish a systematic procedure for measuring the peak quality in each distribution. One option would be to use a Gaussian fit to the peak. Figure 1 illustrates the main difficulty with this option, *i.e.* that invariant mass peaks are anything but Gaussian. One might also consider using the variance of the invariant mass distribution. This, however, fares poorly in reflecting the quality of the peak because of a large sensitivity to the long tails of any distribution. We therefore need to devise peak-quality measures that are independent of any specific functional parametrisation, and truly reflect the nature of the peak itself.

Our logic will be the following. Given two peaks, if they both have similar widths then it is the taller one that is better; if they have similar numbers of events then it is the narrower one that is better. These considerations lead to us to define the two possible measures:

1. $Q_{f=z}^w$: the width of the smallest (reconstructed) mass window that contains a fraction $f = z$ of the generated massive objects,² that is

$$f \equiv \left(\frac{\# \text{ reco. massive objects in window of width } w}{\text{Total } \# \text{ generated massive objects}} \right) = z. \quad (1)$$

A jet definition that is more effective in reconstructing the majority of massive objects within a narrow mass peak gives a lower value for $Q_{f=z}^w$. Therefore smaller values $Q_{f=z}^w$ indicate “better” jet definitions.

²The number of generated massive objects can differ from the total number of events. For example if in the $t\bar{t}$ samples we have $N_{\text{ev}} = 10^5$, the number of generated W bosons (and top quarks) is $N_W = 2 \cdot 10^5$.

Process	# Gen. events	# Acc. events	Fraction acc. vs. gen.	z in eq. (1)
$Z' \rightarrow q\bar{q}$	50 000	$\sim 23\,000$	~ 0.46	0.12
$H \rightarrow gg$	50 000	$\sim 27\,000$	~ 0.54	0.13
Hadronic $t\bar{t}$	100 000	$\sim 75\,000$	~ 0.75	0.18

Table 1: Number of generated events, and those accepted after event selection cuts, together with the fraction of generated events that this corresponds to, and finally the value of z used in eq. (1) (chosen to be roughly 1/4 of the previous column).

Note that we normalise to the total number of generated objects rather than the (smaller) number of objects corresponding to the events that pass the selection cuts. This ensures that we do not favour a jet definition for which only an anomalously small fraction of events pass the selection cuts (as can happen in the $t\bar{t}$ events for large R , where jets are often spuriously merged), even if the JD gives good kinematic reconstruction on that small fraction.

The value of z will be chosen, separately for each process, so that with a typical JD the window contains about 25% of the massive objects in the events that pass the cuts. The values used for z are listed in table 1.

2. $Q_{w=x\sqrt{M}}^{1/f}$: to compute this quality measure, we take a window of fixed width w and slide it over the mass distribution so as to maximise its contents. Then the figure of merit is given by

$$Q_{w=x\sqrt{M}}^{1/f} \equiv \left(\frac{\text{Max \# reco. massive objects in window of width } w = x\sqrt{M}}{\text{Total \# generated massive objects}} \right)^{-1}, \quad (2)$$

where the inverse has been taken so that a better jet definition leads to a smaller $Q_{w=x\sqrt{M}}^{1/f}$, as above. We set the width equal to $x\sqrt{M}$, where M is the nominal heavy object mass and x a constant to be chosen. This reflects the characteristic energy-dependence of resolution in hadronic calorimeters. We take $x = 1.25\sqrt{\text{GeV}}$, a value that is in the ballpark of currently quoted resolutions for the CMS and ATLAS experiments. The reader should be aware that this choice is associated with a degree of arbitrariness.

In tests of a range of possible quality measures for mass reconstructions (including Gaussian fits, and the width at half peak height), the above two choices have been found to be the least sensitive to the precise shape of the reconstructed mass distribution, and have the advantage of being independent of the binning of the distribution. Another encouraging feature, which will be seen below, is that the two measures both lead to similar conclusions on the optimal algorithms and R values.

2.5 Quantitative interpretation of figures of merit

It is useful to establish a relation between variations of the above quality measures and the corresponding variation of integrated luminosity needed to maintain constant significance for a signal relative to background. This will allow us to quantify the importance of any differences between jet definitions (JD) and the potential gain to be had in using the optimal one. The relation will be relevant in the case in which the intrinsic width of the physical resonance that one is trying to

reconstruct is no larger than our (narrow-resonance based) reconstructed dijet-peak — for a very broad physical resonance, the jet-reconstruction quality instead becomes irrelevant.

Our relation will be valid for two background scenarios: one in which the background is flat and independent of the jet definition; and another in which the background is not necessarily flat, but the signal peak and the background shift together as one changes the jet definition (and the second derivative of the background distribution is not too large). For both scenarios, in a window centred on the signal peak, the number of background events will be proportional to the window width, and the constant of proportionality will be independent of the jet definition.

The significance of a signal with respect to the background,

$$\Sigma(\text{JD}) \equiv \frac{N_{\text{signal}}^{\text{JD}}}{\sqrt{N_{\text{bkgd}}^{\text{JD}}}}, \quad (3)$$

where N_{signal} and N_{bkgd} are respectively the number of signal and background events, can then be rewritten as

$$\Sigma(\text{JD}) = \frac{N_{\text{signal}}^{\text{JD}}}{\sqrt{C w^{\text{JD}}}}, \quad (4)$$

where w^{JD} is the width of the window in which we count signal and background events. The argument JD serves as a reminder that the significance will in general depend on the jet definition, and C is a constant independent of the jet definition thanks to our assumptions above on the structure of the background.

We can now establish the following relations between ratios of quality measures for two jet definitions and corresponding ratios of significance. The latter will then relate directly to ratios of luminosities needed to achieve the same significance.

- in the case of $Q_{f=z}^w$ the number of signal events is kept fixed and the window width depends on the jet definition. We have then

$$\frac{\Sigma(\text{JD}_1)}{\Sigma(\text{JD}_2)} = \left[\frac{N_{\text{bkgd}}^{\text{JD}_2}}{N_{\text{bkgd}}^{\text{JD}_1}} \right]^{1/2} = \left[\frac{w^{\text{JD}_2}}{w^{\text{JD}_1}} \right]^{1/2} = \left[\frac{Q_{f=z}^w(\text{JD}_2)}{Q_{f=z}^w(\text{JD}_1)} \right]^{1/2}. \quad (5)$$

- In the case of $Q_{w=x\sqrt{M}}^{1/f}(R)$ the window width is kept constant and it is instead the number of signal events in the window that depends on the jet definition. Hence

$$\frac{\Sigma(\text{JD}_1)}{\Sigma(\text{JD}_2)} = \frac{N_{\text{signal}}^{\text{JD}_1}}{N_{\text{signal}}^{\text{JD}_2}} = \frac{Q_{w=x\sqrt{M}}^{1/f}(\text{JD}_2)}{Q_{w=x\sqrt{M}}^{1/f}(\text{JD}_1)}. \quad (6)$$

Both of these expressions are consistent with the statement that a larger value of a quality measure indicates a worse jet definition (*i.e.* the significance is smaller at fixed integrated luminosity \mathcal{L}). This in turn implies that a larger integrated luminosity will be needed to obtain a given fixed significance. It is convenient to express this in terms of an effective luminosity ratio,

$$\rho_{\mathcal{L}}(\text{JD}_2/\text{JD}_1) \equiv \frac{\mathcal{L}(\text{needed with JD}_2)}{\mathcal{L}(\text{needed with JD}_1)} = \left[\frac{\Sigma(\text{JD}_1)}{\Sigma(\text{JD}_2)} \right]^2. \quad (7)$$

Given a certain signal significance with JD_1 , $\rho_{\mathcal{L}}(\text{JD}_2/\text{JD}_1)$ indicates the factor more luminosity needed to obtain the same significance with JD_2 .³ The expressions for $\rho_{\mathcal{L}}$ in terms of the two quality measures are

$$\rho_{\mathcal{L}}(\text{JD}_2/\text{JD}_1) = \frac{Q_{f=z}^w(\text{JD}_2)}{Q_{f=z}^w(\text{JD}_1)}, \quad (8)$$

and

$$\rho_{\mathcal{L}}(\text{JD}_2/\text{JD}_1) = \left[\frac{Q_{w=x\sqrt{M}}^{1/f}(\text{JD}_2)}{Q_{w=x\sqrt{M}}^{1/f}(\text{JD}_1)} \right]^2. \quad (9)$$

A non-trivial check will be that the luminosity ratios obtained with these two different expressions are consistent with each other. We shall see below that this is generally the case.

3 Results without pileup

Let us start by illustrating the quality measures of section 2.4 for two examples of the processes discussed in section 2.1. Figure 2 shows dijet invariant mass distributions for the 100 GeV $q\bar{q}$ case (upper 6 plots) and the 2 TeV gg case (lower 6 plots). In each case we show 3 different jet definitions. Together with the histograms, we have included a shaded band that represents the region used to calculate the quality measures. In the first and third row we consider $Q_{f=z}^w$ and the quality measure is given by the width of the (cyan) band. In the second and fourth rows, the histograms are the same, but we now show the (dark-green) band used in determining $Q_{w=1.25\sqrt{M}}^{1/f}$ — the quality measure is given by the total number of generated events, divided by the number of events contained in the band.

Within a given row of figure 2 (same process, but different jet definitions), the histograms that “look” best (*i.e.* the rightmost plots) are also those with the smallest quality measures, as should be the case. Furthermore in the situations where one histogram looks only moderately better than another (*e.g.* top row, central and right plots), the values of the quality measures are appropriately close. This gives us a degree of confidence that the quality measures devised in the previous section behave sensibly, and provide a meaningful numerical handle on the otherwise fuzzy concept of “best-looking”.

Before moving on to a more systematic studies of how the quality measures depend on the choice of jet definition, we observe that in figure 2, smaller R gives better results for the 100 GeV $q\bar{q}$ case, while for the the 2 TeV gg case, the opposite happens. This is a concrete illustration of the fact that there is no universal best jet definition.

Next, in figure 3, we show the values of the two quality measures (left: $Q_{f=z}^w$, right $Q_{w=1.25\sqrt{M}}^{1/f}$) for different jet algorithms as a function of R . The top and middle rows correspond to the two processes already studied in figure 2 (100 GeV $q\bar{q}$ and 2 TeV gg), while the bottom row corresponds to top reconstruction in $t\bar{t}$ events. These plots allow one to compare the different jet algorithms, and for each one to determine the radius value that gives the best quality measure. The curves confirm the earlier observation that the 2 TeV gg case prefers a substantially larger choice of R than the 100 GeV $q\bar{q}$ case. To understand this characteristic, it is useful to consider figure 4, which gives the best R (*i.e.* position of the minimum of the quality measure for each algorithm) as a function of momentum scale, separately for the quark and gluon cases. There one sees that for gluonic jets

³Alternatively, for a fixed integrated luminosity, $\sqrt{\rho_{\mathcal{L}}(\text{JD}_2/\text{JD}_1)}$ indicates the extra factor of signal significance that would be gained with JD_1 compared to JD_2 .

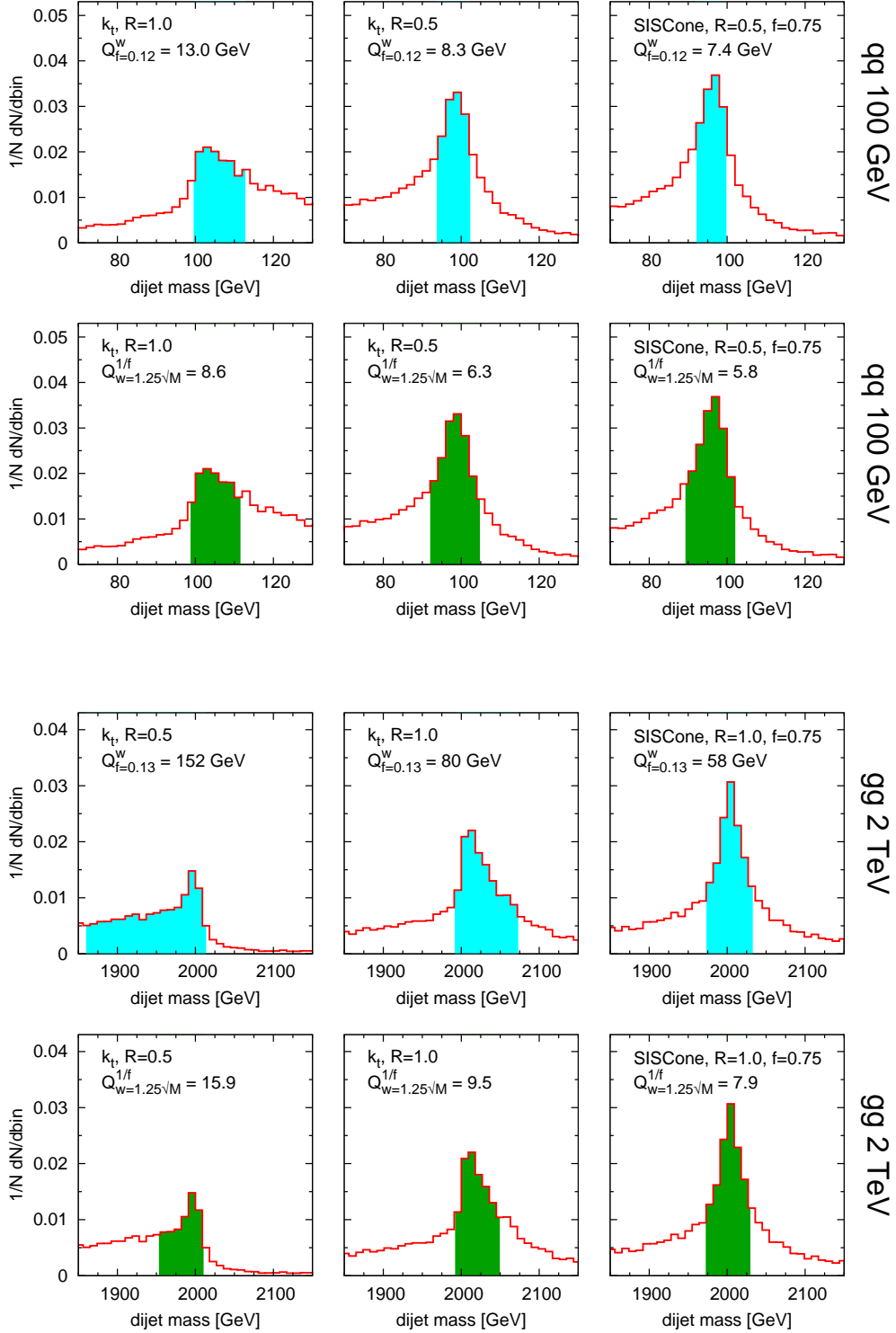


Figure 2: Illustrative dijet invariant mass distributions for two processes (above: $q\bar{q}$ case at $M = 100$ GeV; below: $g\bar{g}$ case at $M = 2$ TeV), comparing three jet definitions for each process. The shaded bands indicate the regions used when obtaining the two different quality measures. Note that different values of R have been used for the $q\bar{q}$ and $g\bar{g}$ cases.

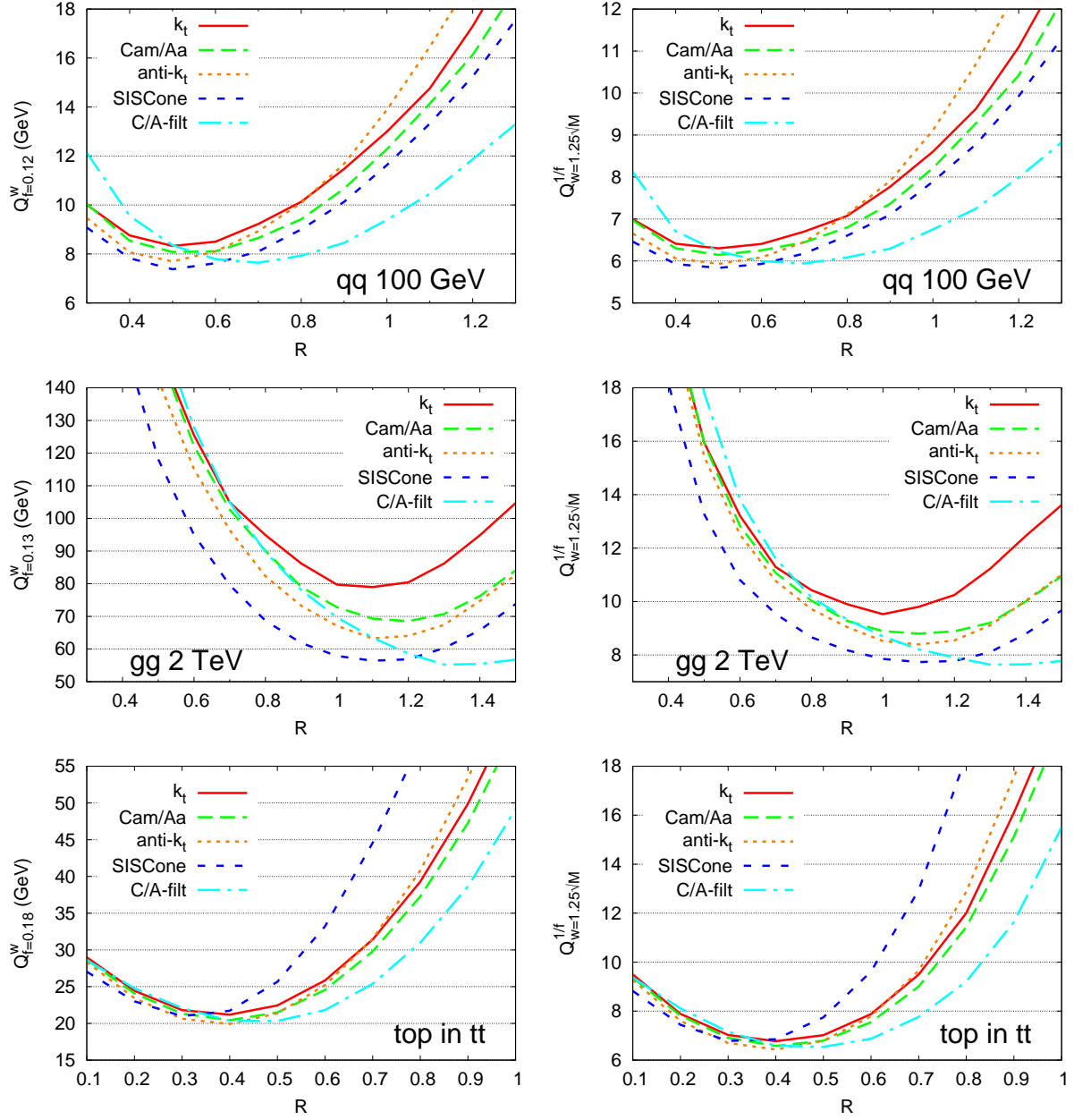


Figure 3: The quality measures $Q_{f=z}^w$ (left) and $Q_{w=1.25\sqrt{M}}^{1/f}$ (right), for different jet algorithms as a function of R , for the 100 GeV $q\bar{q}$ case (top row), 2 TeV $g\bar{g}$ (middle row) and top reconstruction in $t\bar{t}$ events (bottom row).

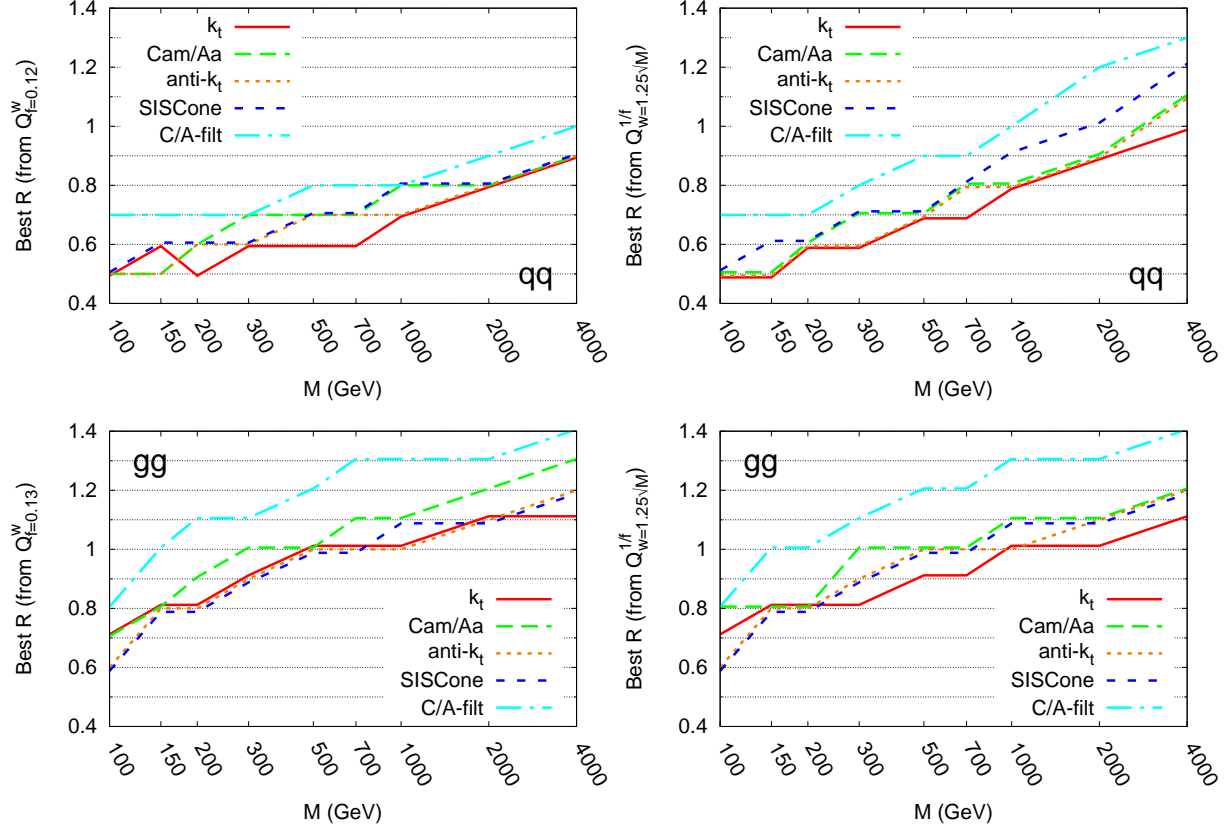


Figure 4: The optimal value for R as a function of the mass of the $q\bar{q}/gg$ system (upper/lower rows), as determined from the two quality measures (left, right columns) for various jet algorithms.

one prefers a larger R than for quark jets, and one also prefers a larger R as one moves to higher momentum scales.

This general pattern was predicted in [20], and is understood in terms of an interplay between the jet needing to capture perturbative radiation, but without excessive contamination from underlying-event (UE) “noise”: whereas perturbative arguments alone would favour R of order 1, the need to limit the amount of UE in the jet pushes one to lower R . The UE matters most relative to the jet energy for low- p_t jets, and perturbative radiation matters more for gluon jets.

A further remark is that the optimal values of R found for processes involving ~ 100 GeV mass scales, $R \sim 0.5$, correspond quite closely to values used typically by the Tevatron experiments and in many LHC studies (see *e.g.* [21, 22]).⁴ Our analysis here confirms that those are therefore good choices. However, at the high scales that will be probed by LHC, ~ 1 TeV, our results indicate that it is important for the experiments to use jet definitions with somewhat larger values of R .

The quantitative impact of a poor choice of jet definition is illustrated in figure 5. For each process, we have identified the jet definition, JD_{best} , that provides the best (lowest) value of the quality measure (*cf.* table 2). Then for every other jet definition, JD , we have calculated the effective increase in luminosity, $\rho_{\mathcal{L}}(JD/JD_{\text{best}})$ as in eq. (7), that is needed to obtain as good a significance as with JD_{best} . This is shown for each jet algorithm as a function of R , with (red) solid lines for

⁴For the Tevatron there will actually be a preference for slightly larger R values than at LHC, a consequence of the more modest UE.

Process	$Q_{f=z}^w$			$Q_{w=1.25\sqrt{M}}^{1/f}$		
	JD _{best}	R	Q (GeV)	JD _{best}	R	Q
$q\bar{q}$, 100 GeV	SISCone	$R=0.5$	7.38	SISCone	$R=0.5$	5.83
$q\bar{q}$, 2 TeV	C/A-filt	$R=0.9$	20.8	SISCone	$R=1.0$	5.18
gg , 100 GeV	SISCone	$R=0.6$	14.7	SISCone	$R=0.6$	8.78
gg , 2 TeV	C/A-filt	$R=1.3$	55.2	C/A-filt	$R=1.3$	7.64
W in $t\bar{t}$	anti- k_t	$R=0.4$	10.7	anti- k_t	$R=0.4$	5.37
t in $t\bar{t}$	anti- k_t	$R=0.4$	19.9	anti- k_t	$R=0.4$	6.44

Table 2: The JD_{best} jet definitions for the various processes of figure 5, together with the corresponding $Q(\text{JD}_{\text{best}})$ values used in calculating $\rho_{\mathcal{L}}$. In the 2 TeV $q\bar{q}$ case, the JD_{best} definitions differ, but figure 5 shows that they lead to very similar quality measures, and the question of which is “best” ultimately depends on fine details of their behaviour.

$Q_{f=z}^w$, using eq. (8), and (blue) dashed lines for $Q_{w=1.25\sqrt{M}}^{1/f}$, using eq. (9).

A first observation is that in general, the two quality measures lead to similar results for $\rho_{\mathcal{L}}$. This is a non-trivial check that the procedure is consistent and that our quality measures behave sensibly.⁵ One should be aware that there is some degree of arbitrariness in the choice of z for $Q_{f=z}^w$ and x for $Q_{w=x\sqrt{M}}^{1/f}$. Accordingly, we have also examined results for the case where these choices are doubled, and verified that $\rho_{\mathcal{L}}$ is again similar (in this respect $Q_{w=x\sqrt{M}}^{1/f}$ seems to be somewhat more stable, *cf.* the web-pages at [6]).

Next, let us discuss the impact of using the worst jet algorithm (at its best R) compared to the best jet definition. At small energy scales one requires about 10 – 20% extra luminosity, a modest effect. At high masses this increases to 30 – 40%. In general it seems that SISCone and C/A-filt are the best algorithms (and are similar to each other), while the k_t algorithm fares worst. In some cases anti- k_t also performs optimally.

The penalty for choosing a non-optimal R can be even larger. For example, using SISCone with $R = 0.4$ (0.5) at 2 TeV leads to $\rho_{\mathcal{L}}$ of about 1.75 (1.35) for the $q\bar{q}$ case, and ~ 3 (2) for the gg case. The use of $R \simeq 0.4 - 0.5$ is widespread in current LHC analyses (for example, [22] used $R = 0.5$ with the CMS iterative cone, which is similar to anti- k_t) and if this is maintained up to high mass scales, it may lead to a need for twice as much integrated luminosity (or even more) to make a discovery as with an optimised choice of jet definition.

A point worth bearing in mind is that the quality measures do not provide all relevant information about the peak. For example, for the small-mass gluonic case, the smallest R values do not lead to appreciably worse-than-optimal $\rho_{\mathcal{L}}$ results, however if one examines the position of the peak (*cf.* the histograms available via the web-tool [6]) one sees that it becomes rather unstable at small R ⁶ [23]. Nevertheless, in most cases, and in particular for all but a few pathological regions of the jet-definition parameter-space, the position of the peak is sensible.

So far we have discussed only simple, dijet events. The last row of figure 3 and the last two rows

⁵In a few instances there are moderate differences between the two determinations of $\rho_{\mathcal{L}}$. This usually occurs when the resulting window widths for the two measures differ substantially (*i.e.* they probe the distribution with different effective resolutions). These cases, however, do not significantly alter any conclusions.

⁶This instability is the cause also of the (somewhat spurious) decrease of $\rho_{\mathcal{L}}$ at small R in the 100 GeV gg C/A-filt case: there, the peak is at quite low masses (~ 50 GeV), and the limited phase-space towards yet-smaller masses causes it to narrow slightly as one further reduces R . Cases like this are rare and easy to identify when they occur.

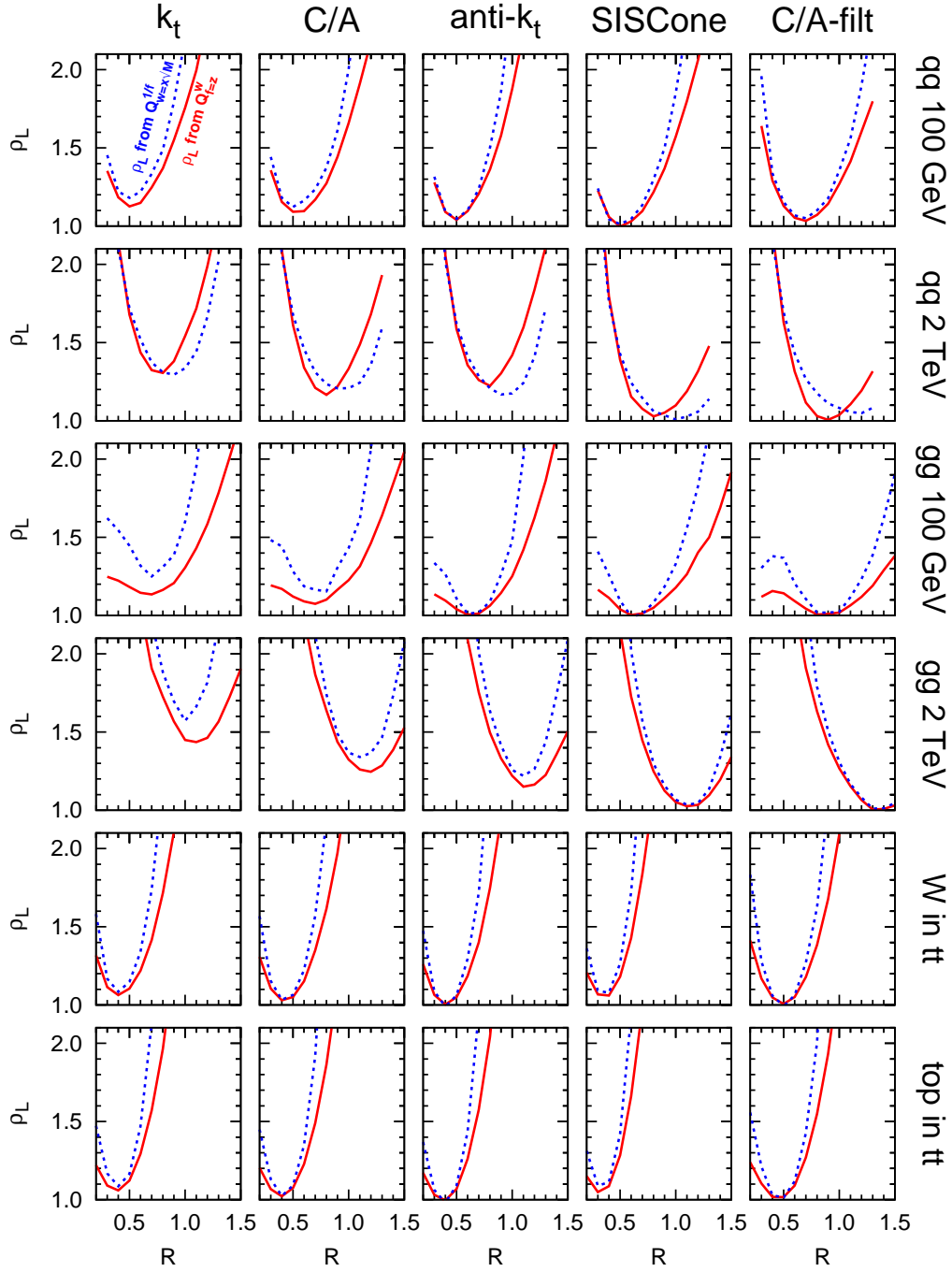


Figure 5: For each process (one per row) this plot shows the luminosity ratio ρ_L required in order to obtain the same significance as with the best jet definition. The (red) solid line corresponds to the estimate of ρ_L from eq. (8) (based on the minimal width $Q_{f=z}^w$), while the (blue) dotted line corresponds to eq. (9) (based on the maximal fraction $Q_{w=1.25\sqrt{M}}^{1/f}$).

of figure 5 show results for more complex $t\bar{t}$ events, which here decay to 6 jets. A first observation is that the optimal R is fairly similar to that in the 100 GeV $q\bar{q}$ case — this is perhaps not surprising, since in both cases the energy of each jet is around 50 GeV. More detailed inspection shows however that the range of “acceptable” R is significantly smaller for the $t\bar{t}$ case than the $q\bar{q}$ case. This is most visible in figure 5, and especially for the SISCone algorithm. The reason is simple: in multijet events, as R is increased, jets that should represent distinct leading-order “partons” may end up being merged.⁷

This issue should be kept in mind when planning analyses involving multijet final states at high energy scales — with current algorithms, there will then be a significant tension between the need for a large radius owing the high energy scale, and the need for a small radius in order to disentangle the many jets. In this respect, methods that use parameters other than just R to resolve jet structure (including some originally intended for jet substructure), such as [24, 25, 26, 17, 27, 28, 29], are likely to be of prime importance in obtaining optimal jet results. The detailed general investigation of such “third-generation” jet-methods⁸ deserves further work.

A final comment concerns studies to reconstruct boosted top quarks, for example from high-mass resonances that decay to $t\bar{t}$ (see *e.g.* [30, 31, 32]). Significant recent work has gone into investigating the identification of top quarks in this context [33, 27, 28, 29, 34], where their decay products are often contained within a single jet. In such a situation, the best R -value for carrying out a top-ID subjet analysis depends on the top p_t , as in [28] (similar to the C/A-based subjet Higgs search of [17]), and is conditioned by the need to take a jet opening angle commensurate with the top-quark dead-cone size and decay angle, $\mathcal{O}(2m_t/p_t)$ ($p_t \sim M/2$ where M is the resonance mass), so that the jet contains the top decay products, but not gluon emission from the top quark itself (which would smear and skew the top mass reconstruction). However, to obtain a good mass-resolution on the high-mass resonance that is reconstructed from the $t\bar{t}$ system, it is instead necessary to *include* any gluon radiation from the top quark inside the jets, and for this purpose, optimal R values will be the larger ones found here for normal $q\bar{q}$ dijet-events and will grow with p_t (this issue obviously does not arise for boosted electroweak bosons). Thus, and in contrast to what has been investigated so far, in the work referred to above, one should work simultaneously with two R values: a small one, $\mathcal{O}(2m_t/p_t)$ for identifying the top-quark decays, and a larger one, as given by figure 4, for determining the top-quark momentum just as it was produced from the resonance decay. In this respect C/A-based solutions (including filtering) are particularly interesting insofar as they allow consistent views of an event at multiple R -values.

4 Results with pileup

It is foreseen that the LHC will operate at a range of different luminosities. One should therefore establish whether the conclusions of the previous section are robust in the presence of multiple minimum-bias (MB) pileup (PU) events. We will consider low and high luminosity scenarios: $\mathcal{L}_{\text{low}} = 0.05 \text{ mb}^{-1}$ and $\mathcal{L}_{\text{high}} = 0.25 \text{ mb}^{-1}$ per bunch crossing,⁹ corresponding respectively to an

⁷SISCone’s higher sensitivity to this effect is a consequence of the fact that for a given R value it can cluster two hard particles that are up to $2R$ apart, whereas the other algorithms reach out only to R .

⁸We use the term “first generation” jet-methods for the infrared and/or collinear unsafe cone algorithms of the ’80s and ’90s, “second generation” for subsequent infrared and collinear safe methods (recombination algorithms like JADE, k_t , C/A and anti- k_t , as well as the cone algorithm SISCone) that essentially use one main fixed parameter to specify the resolution for jets. By third generation methods, we have in mind those that exploit more than a single “view” of the event, and which may be based on a more powerful use of existing algorithms.

⁹Even larger luminosities, $\mathcal{L}_{\text{vhigh}} = 2.5 \text{ mb}^{-1}$, might be relevant at the sLHC upgrade (see for example [35]).

average of about 5 and 25 minimum-bias collisions per bunch crossing (or instantaneous luminosities of $2 \times 10^{33} \text{ cm}^{-2} \text{ s}^{-1}$ and $10^{34} \text{ cm}^{-2} \text{ s}^{-1}$ with a 25 ns bunch spacing). The MB events are simulated using `Pythia` 6.410 [7] with the DWT tune [8], as for our hard event samples, and the number of MB events added to a specific hard event has a Poisson distribution.

It is well known that PU degrades mass resolution and shifts the energy scale, and the LHC experiments will attempt to correct for this. Currently their procedures tend to be highly detector-specific, which limits their applicability in a generic study such as ours. We will therefore use the jet-area-based pileup subtraction method of [36, 16], which is experiment-independent and straightforward to use within the `FastJet` framework.¹⁰ For completeness we give below a quick review of area-based subtraction, and then we will examine the impact of pileup both with and without its subtraction.

4.1 Area-based pileup subtraction

Area-based subtraction involves two elements: the calculation of jet areas, which represent a given jet’s susceptibility to contamination from uniform background noise, and an estimate of the level of background noise in the event.

As proposed in [16], for each jet j in an event, one can determine a 4-vector area in the rapidity-azimuth plane $A_{\mu j}$. Given an estimate for the amount ρ of transverse-momentum per unit area due to background noise, a jet’s corrected (*i.e.* subtracted) momentum $p_{\mu j}^{(\text{sub})}$ is obtained as [36]

$$p_{\mu j}^{(\text{sub})} = p_{\mu j} - A_{\mu j} \rho. \quad (10)$$

Subtracted jets are then used both for event selection and for the mass reconstructions.

The quantity ρ is taken to be independent of rapidity (an acceptable approximation in much of the detector), and calculated on an event-by-event basis as

$$\rho = \text{median} \left\{ \frac{p_{tj}}{A_{tj}} \right\}, \quad (11)$$

where the median is obtained over all jets with $|y| < 5$.¹¹ Regardless of the jet-definition used to analyse the hard event, ρ is always calculated using jets obtained with the k_t algorithm with $R = 0.5$, which choice was found to be particularly robust in [36].¹²

4.2 Results

Jets are most strongly affected by pileup at large R values. Accordingly, in figure 6 we show histograms for the 2 TeV gg process, which without pileup favoured $R \gtrsim 1$. The upper row shows results with no pileup, low and high pileup, all without subtraction. One sees the clear degradation

¹⁰Should the experiments’ internal methods prove to be superior to the jet-area-based method, then the conclusions of this section will only be made more robust; if on the other hand they turn out to perform less well, there would be a compelling reason for them to adopt the area-based method.

¹¹The details of the peak position after subtraction (not the main subject of our study here) can depend on the choice of jets used for calculating ρ , with the issue being largest for large R . As an example, in the 2 TeV gg case with $R = 1$, the residual impact on the peak position can be of order 10 GeV.

¹²Other technical settings are as follows: we use the active area for all jet algorithms except `SISCone`, which for speed reasons we use with the passive area. The area of ghost particles is set to 0.01, they cover the range $|y| < 6$, and the repeat parameter is 1. All other parameters correspond to the defaults in `FastJet` 2.3. For C/A with filtering, the subtraction is carried out before the filtering stage.

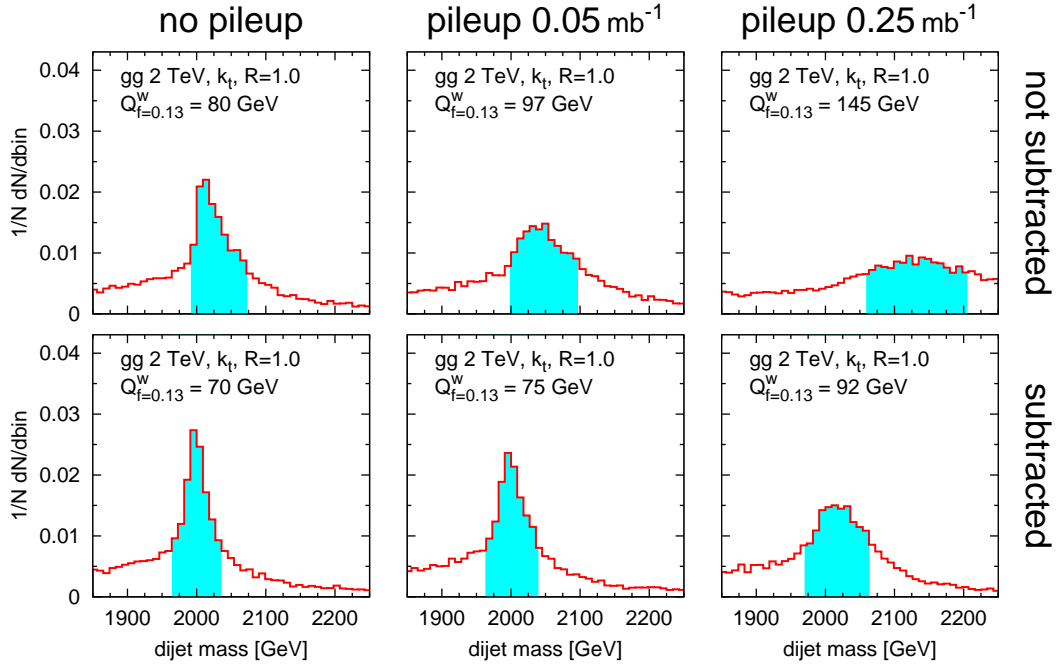


Figure 6: Invariant mass distributions for the 2 TeV gg process, for the k_t algorithm with $R = 1$, shown with no pileup (left), low pileup (middle) and high pileup (right), without subtraction (upper row) and with subtraction (lower row). The shaded bands indicate the region used to calculate the $Q_{f=z}^w$ quality measure in each case.

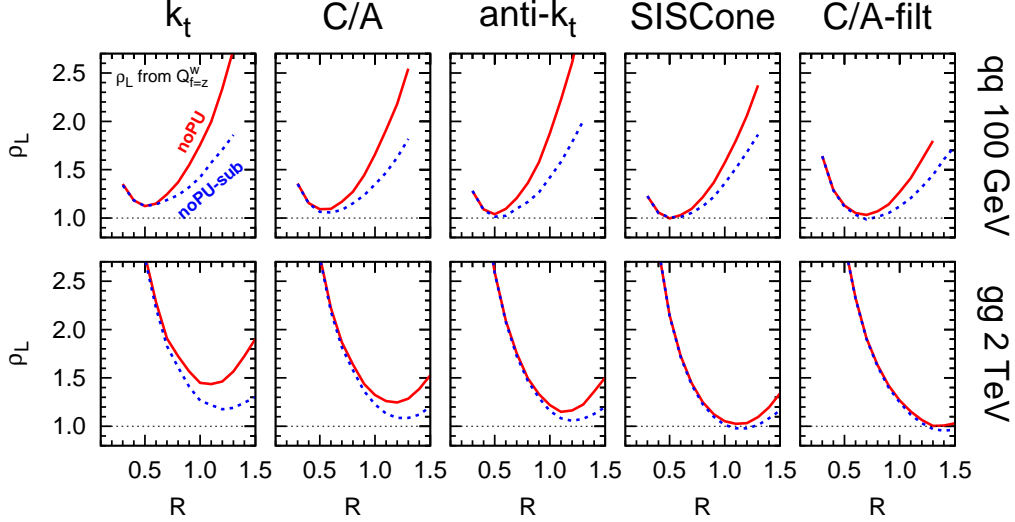


Figure 7: Illustration of the impact of subtraction in the absence of pileup. The effective luminosity ratios are based on the $Q_{f=z}^w$ measure, and normalised to the result for the best jet definition without pileup (no subtraction). The (red) solid curves show results without subtraction, the (blue) dotted curves with subtraction.

in the quality of the peak as pileup is added, and this is reflected in the increasing values of the quality measure. There is additionally a shift of the peak to higher masses.

The lower row of figure 6 shows the corresponding results with subtraction. Note that we have applied subtraction even in the case without pileup and one observes a non-negligible improvement in the peak quality. This is because of the contribution to the “noisiness” of the event from “underlying-event” (UE) activity, which is in part removed by the subtraction procedure. One sees even more significant improvements in the cases with pileup, highlighting the importance of the use of some form of pileup subtraction.

Let us now consider this more systematically. First, in figure 7 we examine the impact of subtraction without pileup for all algorithms for the 100 GeV $q\bar{q}$ and 2 TeV gg processes. This is given in terms of the effective luminosity ratios normalised as in figure 5, *i.e.* to the lowest (best) value of the $Q_{f=z}^w$ quality measure across all jet definitions without pileup (for brevity we omit results based on $Q_{w=1.25\sqrt{M}}^{1/f}$, which do not change the overall conclusions). The (red) solid curve is always the same as in figure 5 (*i.e.* for the jet algorithms without pileup or subtraction), while the (blue) dotted curve shows the results with subtraction. As expected, subtraction only matters significantly at large R . The algorithms that performed worst without subtraction are those that benefit the most from it, leading to quite similar optimal quality for all algorithms.

Next, in figures 8 and 9, we show results respectively for low and high pileup. We maintain the same normalisation for the effective luminosity as before, and the (red) solid curves remain those of figure 5 throughout (no pileup, no subtraction). The (green) dashed curves show the effective luminosity ratios with unsubtracted pileup, while the (blue) dotted curves correspond to subtracted pileup. Unsubtracted pileup, unsurprisingly, degrades the quality in almost all cases, more so at larger R values. This R -dependence of the quality degradation causes the minima to shift to moderately smaller R values. Subtraction compensates for part of the loss of quality (and the shift in best R) due to pileup, though to an extent that varies according to the case at hand.

For the purpose of this article, the main conclusion from figures 8 and 9 is that, if one chooses

a jet-definition that is optimal in the case without pileup (*i.e.* based on the results of section 3), then in the presence of pileup (with subtraction) it gives a $\rho_{\mathcal{L}}$ that remains within about 10% of the lowest possible value. Insofar as a given analysis may involve data taken at a range of instantaneous luminosities (which may even vary significantly over the lifetime of the beam), this is important since it implies that it will be satisfactory to choose a single jet-definition independently of the level of pileup.

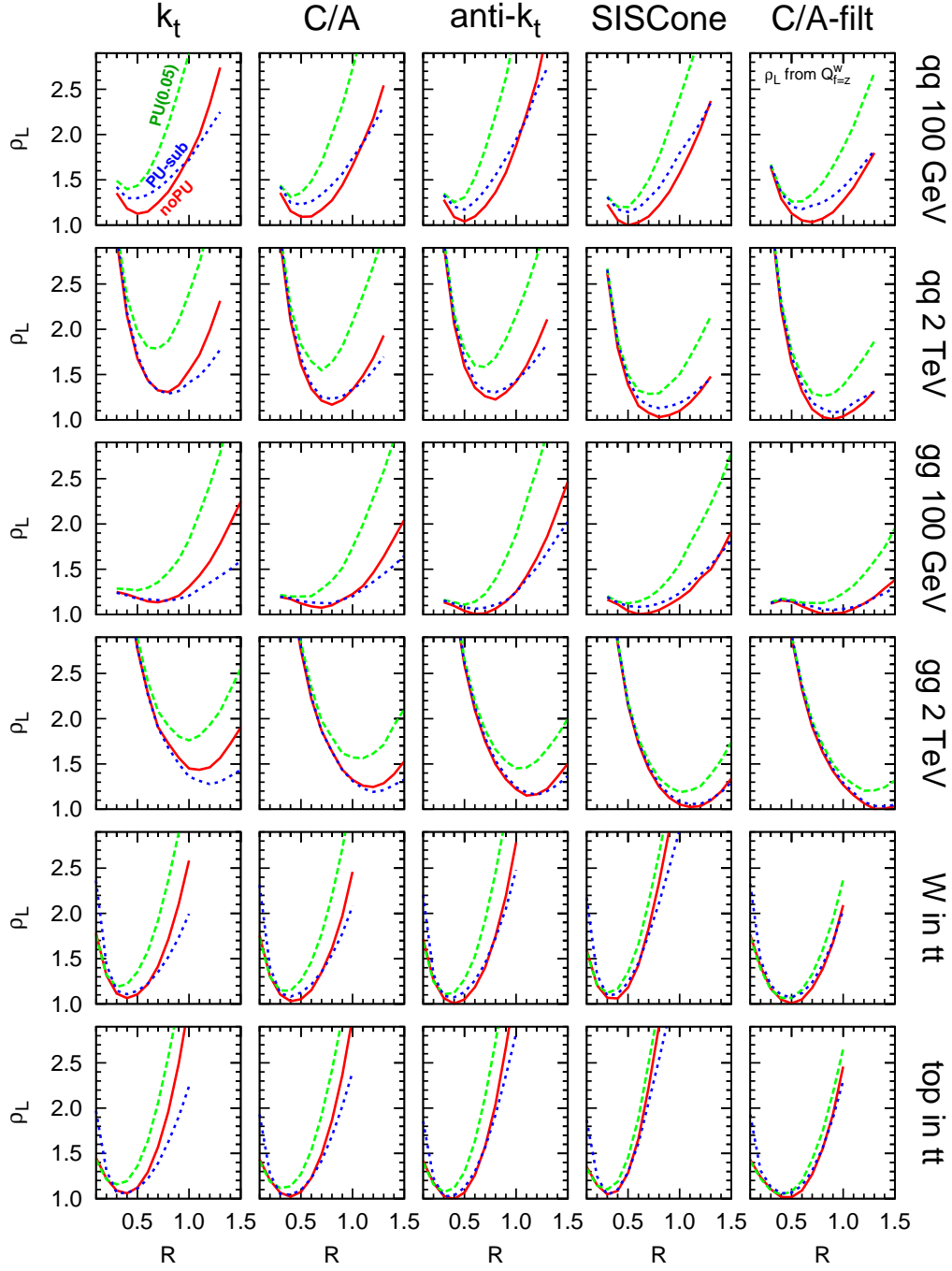


Figure 8: Illustration of the impact of low pileup, 0.05 mb^{-1} per bunch crossing. Luminosity ratios have been calculated based on the $Q_{f=z}^w$ measure, and normalised to the result for the best jet definition without pileup (no subtraction). The (red) solid curves show the result with no pileup and no subtraction, the (green) dashed curves have pileup without subtraction and the (blue) dotted curves have pileup and subtraction.

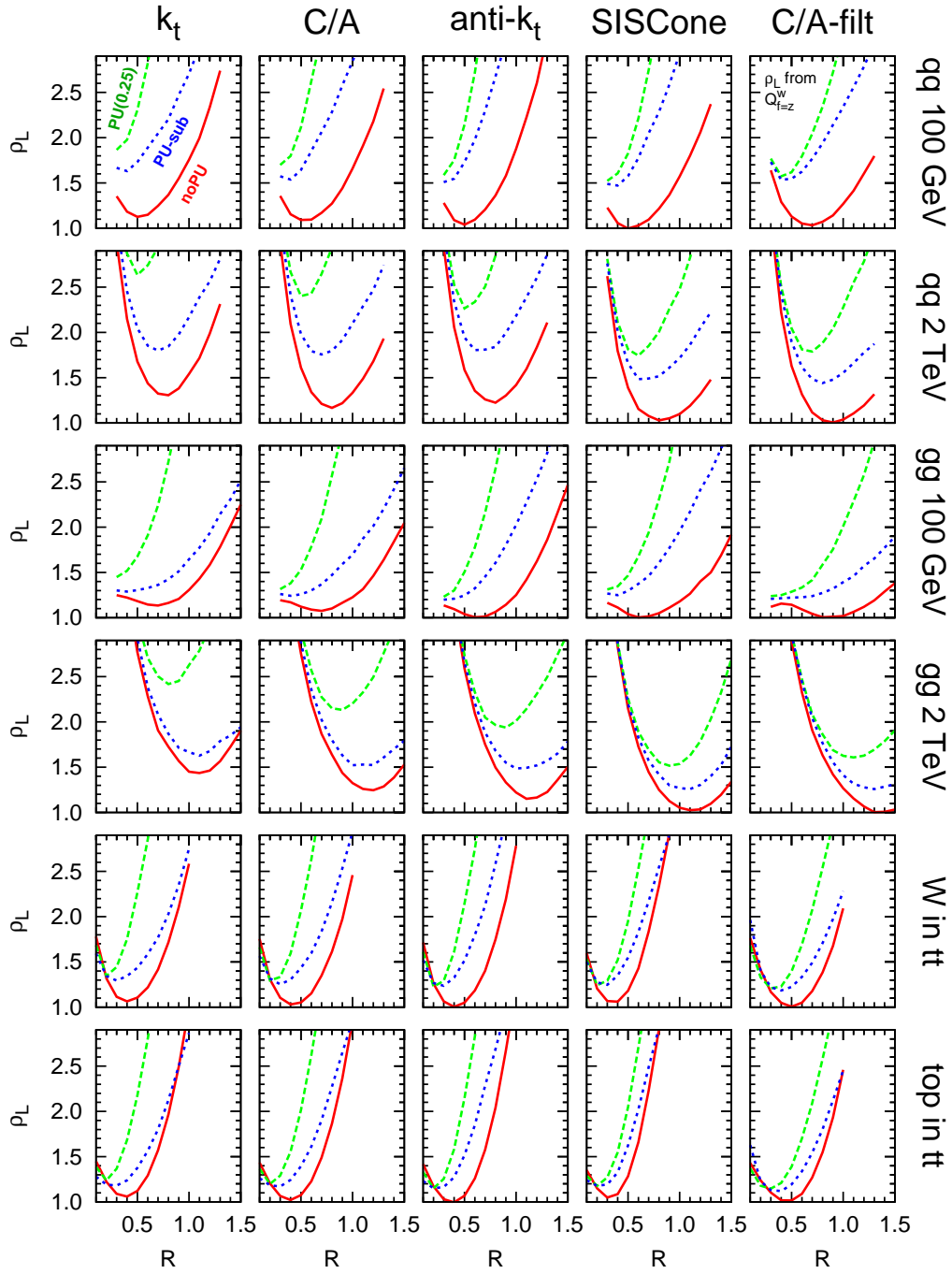


Figure 9: As in figure 8, but for high luminosity, 0.25 mb^{-1} per bunch crossing.

5 Conclusions

In this paper, we have examined the question of assessing the relative quality of a range of jet definitions for kinematic reconstructions. In contrast to other common approaches, we chose not to determine the quality of a jet definition in terms of how well its jets correspond to a given (but ill-defined) set of hard Monte-Carlo partons. Instead we used physically well-defined measures, *i.e.* the reconstruction of an invariant (dijet or top) mass peak. The quality of a given jet-definition is then related to the “sharpness” of the mass peak. Since sharpness is a somewhat fuzzy concept we introduced two “quality measures” to quantify the concept, independently of the peak shape, which is usually strongly non-Gaussian. With certain hypotheses, one can establish a proportionality relation between these quality measures and the amount of integrated luminosity needed to obtain a given statistical significance in a search.

We studied the cases of narrow $q\bar{q}$ and gg resonances over mass scales ranging from 100 GeV to 4 TeV, as well as top and W reconstruction in $t\bar{t}$ events. We considered 5 jet algorithms, k_t , Cambridge/Aachen (C/A), anti- k_t , SIS Cone¹³ and C/A with filtering, over jet-radii, R , spanning typically from 0.3 to 1.3.

Our results (available in a more extensive form via the online tool [6]) tend to validate the existing widespread use of low radii 0.4 – 0.5 in reconstructing quark-induced jets at mass scales of $\mathcal{O}(100 \text{ GeV})$. However they also show that gluon-induced jets and high-scale jets prefer significantly larger R , up to an optimal value of $R \sim 1.2$ for the high-mass gg case. This general pattern coincides broadly with analytical expectations [20], and relates to an interplay between needing to capture perturbative radiation from the jet, while excluding underlying-event contamination. The former matters more at high scales and for gluon jets, hence the preference for larger R .

A second pattern that emerges, relevant mainly at higher energy scales, is that among traditional (or “second generation,” *cf.* footnote 8) types of jet algorithm, SIS Cone often performs best and anti- k_t performs better than other sequential recombination algorithms, k_t and C/A. The third-generation C/A-filtering algorithm typically performs as well as SIS Cone, but prefers slightly larger R . Both SIS Cone and C/A-filtering’s good performance can be traced back to their low sensitivity to underlying-event activity.

A quantitative presentation of these results is given in figure 5, for a subset of processes, in terms of the extra factor in integrated luminosity that would be needed for a given jet definition to achieve the same significance as the optimal one in our set. An implication for LHC experiments planning to use $R = 0.4 - 0.6$ even in large-mass searches (see *e.g.* [21, 22]), is that some discoveries may then require up to twice more integrated luminosity than would be the case with the optimal choice of jet-definition.

Given such a statement, it is important to establish how it is affected by pileup. This was the subject of section 4. The conclusions are that the optimal jet definition without pileup remains close to optimal even with high-luminosity pileup (*i.e.* with ~ 25 pp interactions per bunch crossings), provided that adequate subtraction methods are used to correct the jets for the pileup. Subtraction also reduces the differences between jet algorithms, even in the absence of pileup, *cf.* figure 7.

Finally, given that the bulk of our results apply to dijet events, one may ask to what extent they hold in multi-jet situations. To investigate this, we have studied hadronic $t\bar{t}$ events and observed results similar to those for the low-mass $q\bar{q}$ case. However, we envisage that in multi-jet events at high mass scales there will be an additional tension between the need to resolve the separate

¹³ We recall that anti- k_t is expected to behave similarly to iterative cones with progressive removal (like the current CMS iterative cone), while being infrared and collinear (IRC) safe. SIS Cone is an IRC safe cone algorithm with a split–merge step, and is therefore closer to iterative cone algorithms like the current ATLAS cone.

jets and the need to include the bulk of perturbative gluon emission in the jet. The study of the issue is beyond the scope of this article, but we foresee that future developments in third-generation jet-methods can play an important role in optimising analyses of such events.

Acknowledgements

This work has been supported in part by the grant ANR-05-JCJC-0046-01 from the French Agence Nationale de la Recherche and under Contract No. DE-AC02-98CH10886 with the U.S. Department of Energy, and was started at 2007 Physics at TeV Colliders Les Houches workshop. It is a pleasure to acknowledge interesting discussions with A. Oehler and K. Rabbertz, we are grateful to G. Dissertori and G. Zanderighi for comments on the manuscript, and JR thanks D. d’Enterria for a useful conversation. GPS wishes to thank Brookhaven National Laboratory and Princeton University for hospitality while this work was being completed.

References

- [1] C. Buttar *et. al.*, *Standard Model Handles and Candles Working Group: Tools and Jets Summary Report*, [arXiv:0803.0678](#).
- [2] S. Frixione and B. R. Webber, *Matching NLO QCD computations and parton shower simulations*, *JHEP* **06** (2002) 029, [[hep-ph/0204244](#)].
- [3] P. Nason, *A new method for combining NLO QCD with shower Monte Carlo algorithms*, *JHEP* **11** (2004) 040, [[hep-ph/0409146](#)].
- [4] A. Santocchia, *Optimization of Jet Reconstruction Settings and Parton-Level Correction for the $t\bar{t}H$ Channel*, tech. rep., 2006. CERN-CMS-NOTE-2006-059.
- [5] A. P. Cheplakov and S. Thompson, *MidPoint Algorithm for Jets Reconstruction in ATLAS Experiment*, tech. rep., 2007. ATL-PHYS-PUB-2007-007.
- [6] M. Cacciari, J. Rojo, G. P. Salam, and G. Soyez, <http://quality.fastjet.fr/>.
- [7] T. Sjöstrand, S. Mrenna, and P. Skands, *Pythia 6.4 physics and manual*, *JHEP* **05** (2006) 026, [[hep-ph/0603175](#)].
- [8] M. G. Albrow *et. al.*, *Tevatron-for-LHC report of the QCD working group*, [hep-ph/0610012](#).
- [9] S. Catani, Y. L. Dokshitzer, M. Olsson, G. Turnock, and B. R. Webber, *New clustering algorithm for multi - jet cross-sections in e^+e^- annihilation*, *Phys. Lett.* **B269** (1991) 432–438.
- [10] S. Catani, Y. L. Dokshitzer, M. H. Seymour, and B. R. Webber, *Longitudinally invariant k_t clustering algorithms for hadron hadron collisions*, *Nucl. Phys.* **B406** (1993) 187–224.
- [11] S. D. Ellis and D. E. Soper, *Successive combination jet algorithm for hadron collisions*, *Phys. Rev.* **D48** (1993) 3160–3166, [[hep-ph/9305266](#)].
- [12] Y. L. Dokshitzer, G. D. Leder, S. Moretti, and B. R. Webber, *Better jet clustering algorithms*, *JHEP* **08** (1997) 001, [[hep-ph/9707323](#)].

- [13] M. Wobisch and T. Wengler, *Hadronization corrections to jet cross sections in deep- inelastic scattering*, [hep-ph/9907280](#).
- [14] M. Cacciari, G. P. Salam, and G. Soyez, *The anti- k_t jet clustering algorithm*, *JHEP* **04** (2008) 063, [[arXiv:0802.1189](#)].
- [15] G. P. Salam and G. Soyez, *A practical seedless infrared-safe cone jet algorithm*, *JHEP* **05** (2007) 086, [[arXiv:0704.0292](#)].
- [16] M. Cacciari, G. P. Salam, and G. Soyez, *The Catchment Area of Jets*, *JHEP* **04** (2008) 005, [[arXiv:0802.1188](#)].
- [17] J. M. Butterworth, A. R. Davison, M. Rubin, and G. P. Salam, *Jet substructure as a new Higgs search channel at the LHC*, *Phys. Rev. Lett.* **100** (2008) 242001, [[arXiv:0802.2470](#)].
- [18] M. Cacciari and G. P. Salam, *Dispelling the N^3 myth for the k_t jet-finder*, *Phys. Lett.* **B641** (2006) 57–61, [[hep-ph/0512210](#)].
- [19] M. Cacciari, G. P. Salam, and G. Soyez, <http://www.fastjet.fr/> .
- [20] M. Dasgupta, L. Magnea, and G. P. Salam, *Non-perturbative QCD effects in jets at hadron colliders*, *JHEP* **02** (2008) 055, [[arXiv:0712.3014](#)].
- [21] S. D. Ellis, J. Huston, K. Hatakeyama, P. Loch, and M. Tonnesmann, *Jets in Hadron-Hadron Collisions*, *Prog. Part. Nucl. Phys.* **60** (2008) 484–551, [[arXiv:0712.2447](#)].
- [22] A. Bhatti *et. al.*, *CMS search plans and sensitivity to new physics with dijets*, [arXiv:0807.4961](#).
- [23] One of us (GPS) wishes to thank A. Oehler and K. Rabbertz for a discussion related to this point.
- [24] J. M. Butterworth, B. E. Cox, and J. R. Forshaw, *W W scattering at the LHC*, *Phys. Rev.* **D65** (2002) 096014, [[hep-ph/0201098](#)].
- [25] M. H. Seymour and C. Tevlin, *A comparison of two different jet algorithms for the top mass reconstruction at the LHC*, *JHEP* **11** (2006) 052, [[hep-ph/0609100](#)].
- [26] J. M. Butterworth, J. R. Ellis, and A. R. Raklev, *Reconstructing sparticle mass spectra using hadronic decays*, *JHEP* **05** (2007) 033, [[hep-ph/0702150](#)].
- [27] J. Thaler and L.-T. Wang, *Strategies to Identify Boosted Tops*, *JHEP* **07** (2008) 092, [[arXiv:0806.0023](#)].
- [28] D. E. Kaplan, K. Rehermann, M. D. Schwartz, and B. Tweedie, *Top-tagging: A Method for Identifying Boosted Hadronic Tops*, [arXiv:0806.0848](#).
- [29] L. G. Almeida *et. al.*, *Substructure of high- p_T Jets at the LHC*, [arXiv:0807.0234](#).
- [30] K. Agashe, A. Belyaev, T. Krupovnickas, G. Perez, and J. Virzi, *LHC signals from warped extra dimensions*, *Phys. Rev.* **D77** (2008) 015003, [[hep-ph/0612015](#)].
- [31] B. Lillie, L. Randall, and L.-T. Wang, *The Bulk RS KK-gluon at the LHC*, *JHEP* **09** (2007) 074, [[hep-ph/0701166](#)].

- [32] U. Baur and L. H. Orr, *Searching for t -bar t Resonances at the Large Hadron Collider*, *Phys. Rev.* **D77** (2008) 114001, [[arXiv:0803.1160](#)].
- [33] G. Broojimans, High p_t hadronic top quark identification part I: Jet mass and ysplitter. ATL-PHYS-CONF-2008-08.
- [34] L. G. Almeida, S. J. Lee, G. Perez, I. Sung, and J. Virzi, *Top Jets at the LHC*, [arXiv:0810.0934](#).
- [35] <http://care-hhh.web.cern.ch/CARE-HHH/upgradetable.pdf> .
- [36] M. Cacciari and G. P. Salam, *Pileup subtraction using jet areas*, *Phys. Lett.* **B659** (2008) 119–126, [[arXiv:0707.1378](#)].